A model for the high-temperature transport properties of heavily doped *n*-type silicon-germanium alloys

Cronin B. Vining
Jet Propulsion Laboratory, California Institute of Technology, Pasadena, California 91109-8099

(Received 6 April 1990; accepted for publication 11 September 1990)

A model is presented for the high-temperature transport properties of large-grain-size, heavily doped *n*-type silicon-germanium alloys. Electron and phonon transport coefficients are calculated using standard Boltzmann equation expressions in the relaxation time approximation. Good agreement with experiment is found by considering acoustic phonon and ionized impurity scattering for electrons, and phonon-phonon, point defect, and electron-phonon scattering for phonons. The parameters describing electron transport in heavily doped and lightly doped materials are significantly different and suggest that most carriers in heavily doped materials are in a band formed largely from impurity states. The maximum dimensionless thermoelectric figure of merit for single-crystal, *n*-type $Si_{0.8}Ge_{0.2}$ at 1300 K is estimated at $ZT \simeq 1.13$ with an optimum carrier concentration of $n \simeq 2.9 \times 10^{20}$ cm^{-3}.

I. INTRODUCTION

The discovery that the thermal conductivity of silicon-germanium alloys was much lower than predicted by linear interpolation[1] spurred interest in these materials for thermoelectric applications. The thermoelectric properties of SiGe alloys were studied in the 1960s as a function of composition, carrier concentration, and temperature using heavily doped zone-leveled materials.[2,3] Prepared by more economical powder metallurgical techniques,[4,5] these alloys are still in use today as the active elements in radioisotope thermoelectric generators[6,7] (RTGs), providing reliable electrical power for the Voyager and, more recently, the Galileo spacecrafts. The ability to tailor the material properties through alloying and the extensive background information available has resulted in continuing interest in modifications of SiGe alloys such as thin films,[8-10] amorphous materials[11,12] and hot-pressed materials.[5,13-16]

Various efforts to improve the thermoelectric performance of SiGe alloys have also been reported. Addition of GaP, once thought to lower the thermal conductivity,[17] is now believed to act as a superior dopant.[14,15] Theoretical calculations indicating improved figure-of-merit values for hot-pressed SiGe alloys due to grain-boundary scattering of phonons[18,19] have been partially verified: Hot-pressed SiGe alloys have been shown to have lower thermal conductivity values,[20,21] but only modest (11% or less) enhancements in figure-of-merit values have been reported[5,22] due to offsetting reductions in the electrical conductivity.

In consideration of the continued interest in SiGe alloys and ongoing efforts to improve their thermoelectric figure-of-merit values, better theoretical models of their transport properties would be very useful, particularly at high carrier concentrations and temperatures. Space applications such as RTGs can particularly benefit from improved theoretical guidelines. Even modest improvements in thermoelectric performance can result in substantial savings due to the high cost of fuels for RTGs.

The most complete study in the literature which attempts to describe all of the transport properties of heavily doped SiGe alloys is due to Raag.[23-25] In this work the electrical resistivity and thermal conductivity of hot-pressed $Si_{78}Ge_{22}$ was studied experimentally as a function of time and temperature for periods of up to 4000 h. The Seebeck coefficient values were estimated from the measured resistivity values, using prior experimental data on zone-leveled SiGe. The results as a function of time and temperature were summarized in graphical form and later were reduced to tables for use in a computer look-up scheme.[26]

This work has proven extremely useful for engineering applications, but is not actually a model since both the transport properties and the precipitation kinetics were treated essentially empirically. Only one attempt to simultaneously model both the mobility and Seebeck coefficient of heavily doped SiGe alloys has been published, but the results were only qualitatively reliable.[27] Calculations of the electrical mobility have been performed for undoped SiGe alloys, including alloy disorder scattering of the electrons,[28] but this work has not been extended to doped materials.

A detailed model for the mobility of *n*-type silicon has been reported by Li and Thurber,[29] covering carrier densities approaching 10^{20} cm^{-3}. In addition to acoustic-phonon and ionized-impurity scattering mechanisms, Li and Thurber considered scattering due to several different optical phonons, scattering due to unionized impurities, and attempted to account for electron-electron interactions. Agreement with mobilities at the highest doping levels is still not remarkable, and no attempt has been made to calculate other transport coefficients.

Published models for the lattice thermal conductivity of SiGe alloys, while yielding better agreement with experiment than models for the electrical properties, nevertheless require adjustment of at least one parameter for each doping level[30] or adjustment of a parameter for each temperature.[3] In particular, no published model has simultaneously accounted for the high-temperature Seebeck coefficient (Q), electrical resistivity (ρ), Hall mobility, and thermal conductivity.

 0021-8979/91/010331-11$03.00

This paper describes a predictive, quantitative, theoretically justifiable and self-consistent model of all of the thermoelectric properties of heavily doped silicon-germanium alloys, neglecting the effects of grain boundaries and phonon drag. Section II describes the quantities used in the model. Sections III and IV describe the details of the electrical and lattice contributions to the transport coefficients, and Sec. V describes the numerical procedures used. Comparison to experimental results and discussion of the results are given in Secs. VI and VII.

II. CLASSIFICATION OF QUANTITIES USED IN THE MODEL

The quantities used in this model are classified according to their role in the calculations. Six kinds of quantities are distinguished: physical constants, independent variables, dependent parameters, adjustable parameters, unobserved dependent variables, and observed transport coefficients. This classification scheme, summarized in Table I, is somewhat arbitrary, but helps to emphasize important differences in the way various quantities are handled.

The physical constants have their usual meanings. The dependent parameters are material properties which can be unambiguously calculated from the two independent parameters y and T alone. The values of the dependent parameters have been selected to accurately model the functional dependence of these quantities.

The adjustable parameters are quantities which are to be determined by comparison to experiment. With the exception of the chemical potential, a single set of values for the adjustable parameters is expected to describe the transport properties of SiGe alloys over the entire range of compositions, temperature, and doping level of interest. Treating the chemical potential (or some equivalent choice, such as N_d) as an adjustable parameter is an unavoidable complication which will be discussed in detail in Sec. VII.

The observable transport coefficients are those properties which can be directly determined by experiment. Since ρ, μ_H, and R_H are not independent of each other, any two coefficients may be equivalently treated as observable, but not all three. Other quantities of interest, such as the lattice thermal conductivity and minority-carrier contributions to the electronic transport coefficients, are classified as unobserved dependent variables. This nomenclature serves as a reminder that only *total* transport coefficients are actually observed, and estimation of the various contributions to such quantities can be highly model dependent.

III. ELECTRICAL MODEL

For this work, the relaxation time approximation of Boltzmann's equation[32] has been adopted. This method is in common use, allows calculation of all of the transport coefficients, and is relatively simple to implement. Full account is taken of Fermi statistics, and minority-carrier effects are approximated. Two scattering mechanisms for the electrons are considered: (1) scattering by acoustic lattice vibrations and (2) scattering by ionized impurities.

TABLE I. Classification of quantities used in the model.

Physical constants	
e = magnitude of charge on an electron	
m_e = mass of the electron	
k_B = Boltzmann's constant	
h = Planck's constant	
$\hbar = h/2\pi$	
N_A = Avogadro's number	
Independent variables	
y = germanium content ($Si_{1-y}Ge_y$)	
T = temperature	
Dependent parameters	
$a^3 = (2.7155\ \text{Å})^3(1-y) + (2.8288\ \text{Å})^3 y$	mean atomic volume
$\Delta a = 2.8288 - 2.7155$ Å	atomic size difference
$M = 28.086\,(1-y) + 72.59\,y$	mean atomic mass
$\Delta M = 72.59 - 28.086$	mass difference
$d = M/a^3$	mass density
$G = 1.033\,(1-y) + 1.017\,y$	related to elastic constants[a]
$\theta = 1.48\times10^{-8} a^{-3/2} M^{-1/2} G$	Debye temperature[a]
$v = \frac{k_B}{\hbar}(6\pi^2)^{-1/3}\theta a$	speed of sound
$E_g = 0.8941 + 0.0421(1-y) + 0.1961\,(1-y)^2 - [0.00037\,y + 0.00023\,(1-y)]$	band-gap energy[b]
$E_g^* = E_g/k_B T$	reduced band-gap energy
Adjustable parameters	
Literature values:	
$\beta = 2.0$,	the ratio of Normal and Umklapp scattering rates[a]
$\gamma = 0.91$	the anharmonicity parameter[a]
$\epsilon_s = 39$	a strain parameter for point defect scattering[a]
This study:	
$m_\pm = 1.40\,m_e$	effective mass of a charge carrier[c]
$E_\pm = 2.94$ eV	deformation potential[c]
$\epsilon_\pm = 27.4$	dielectric constant[c]
$\eta^* = \eta/k_B T$	reduced chemical potential of an electron
Unobserved dependent variables	
$T^*_{v\pm}$ = reduced carrier energy, at the speed of sound	
$n^\pm$ = density of charge carriers in each band	
N_d = density of ionized electron donors	
$\sigma^\pm$ = partial electrical conductivity of each band	
$R_H^\pm$ = partial Hall coefficient for each band	
R_H = total Hall coefficient	
$\mu_H^\pm$ = partial Hall mobility for each band	
$Q^\pm$ = partial Seebeck coefficient for each band	
$\mathscr{L}^\pm$ = partial Lorentz factor for each band	
$\mathscr{L}$ = total Lorentz factor	
$K_e = \mathscr{L}\sigma T$ = electronic contribution to the thermal conductivity	
K_l = lattice contribution to the thermal conductivity	
$ZT = Q^2\sigma T/K$ = thermoelectric figure of merit	
$x = \mathscr{E}/k_B T$ = reduced energy of electrons or phonons	
Observable transport coefficients	
σ = total electrical conductivity	
Q = total Seebeck coefficient	
μ_H = total Hall mobility	
$K = K_e + K_l$ = total thermal conductivity	

[a] Reference 30.
[b] Reference 31.
[c] This study.

The concentration of electrons, n^-, is given by

$$n^- = 4\pi\left(\frac{2m_- k_B T}{h^2}\right)^{3/2} F_{1/2}(\eta^*) \tag{1}$$

where η^* is the reduced chemical potential (relative to the conduction-band edge) and $F_{1/2}(\eta^*)$ is a Fermi integral of the type

$$F_n(\eta^*) = \int_0^\infty \frac{x^n dx}{1+\exp(x-\eta^*)}. \tag{2}$$

The electrical conductivity of the electrons is calculated by taking an appropriate average of the relaxation time and is given by

$$\sigma^- = \frac{8\pi e^2}{3m_- h^3}(2m_- k_B T)^{3/2} G^-_{3/2}(\eta^*), \tag{3}$$

where $G^-_{3/2}(\eta^*)$ represents an average of the relaxation time given by

$$G^\pm_n(\eta^*) = \int_0^\infty \frac{\tau^\pm x^n \exp(x-\eta^*)dx}{[1+\exp(x-\eta^*)]^2}, \tag{4}$$

and $\tau^\pm$ is the appropriate scattering rate, + and − indicating holes and electrons, respectively. Similarly, the Seebeck coefficient due to the electrons is given by

$$Q^- = -\frac{k_B}{e}\left(\frac{G^-_{5/2}(\eta^*)}{G^-_{3/2}(\eta^*)} - \eta^*\right). \tag{5}$$

The Hall coefficient involves a slightly different average of the relaxation time and is given by

$$R^-_H = -\frac{3h^3}{8\pi e(2m_- k_B T)^{3/2}} \frac{H^-_{3/2}(\eta^*)}{(G^-_{3/2})^2(\eta^*)}, \tag{6}$$

where

$$H^\pm_n(\eta^*) = \int_0^\infty \frac{(\tau^\pm)^2 x^n \exp(x-\eta^*)dx}{[1+\exp(x-\eta^*)]^2}. \tag{7}$$

The final transport coefficient of interest here is the Lorenz number,

$$\mathcal{L}^- = \left(\frac{k_B}{e}\right)^2\left(\frac{G^-_{3/2}(\eta^*)G^-_{7/2}(\eta^*) - (G^-_{5/2})^2(\eta^*)}{(G^-_{3/2})^2(\eta^*)}\right), \tag{8}$$

which is needed to calculate the electronic contribution to the thermal conductivity.

Similar expressions are used for the transport coefficients of the holes. The only changes are the substitution of a relaxation time appropriate to holes, the use of a generally different effective mass for the holes, and the substitution of $(-\eta^* - E_g^*)$ for η^* in the various transport integrals.

Thus, the expressions for the properties of the holes are

$$n^+ = 4\pi\left(\frac{2m_+ k_B T}{h^2}\right)^{3/2} F_{1/2}(-E_g^* - \eta^*), \tag{9}$$

$$\sigma^+ = \frac{8\pi e^2}{3m_+ h^3}(2m_+ k_B T)^{3/2} G^+_{3/2}(-E_g^* - \eta^*), \tag{10}$$

$$R^+_H = \frac{3h^3}{8\pi e(2m_+ k_B T)^{3/2}} \frac{H^+_{3/2}(-E_g^* - \eta^*)}{(G^+_{3/2})^2(-E_g^* - \eta^*)}, \tag{11}$$

$$Q^+ = \frac{k_B}{e}\left(\frac{G^+_{5/2}(-E_g^* - \eta^*)}{G^+_{3/2}(-E_g^* - \eta^*)} + E_g^* + \eta^*\right), \tag{12}$$

$$\mathcal{L}^+ = \left(\frac{k_B}{e}\right)^2\left(\frac{G^+_{3/2}(-E_g^* - \eta^*)G^+_{7/2}(-E_g^* - \eta^*) - (G^+_{5/2})^2(-E_g^* - \eta^*)}{(G^+_{3/2})^2(-E_g^* - \eta^*)}\right). \tag{13}$$

The electron and hole contributions are combined to yield the various total transport coefficients. The net number of ionized impurities is given by the charge neutrality condition

$$N_d = n^- - n^+. \tag{14}$$

The total electrical conductivity, Seebeck coefficient, Hall coefficient, Hall mobility, and Lorentz number are given by

$$\sigma = \sigma^+ + \sigma^-, \tag{15}$$

$$Q = (Q^+\sigma^+ + Q^-\sigma^-)/\sigma, \tag{16}$$

$$R_H = [R^+_H(\sigma^+)^2 + R^-_H(\sigma^-)^2]/\sigma^2, \tag{17}$$

$$\mu_H = \sigma R_H, \tag{18}$$

and

$$\mathcal{L} = \left(\mathcal{L}^+\sigma^+ + \mathcal{L}^-\sigma^- + \frac{\sigma^+\sigma^-}{\sigma}(Q^+ - Q^-)^2\right)\sigma, \tag{19}$$

respectively. The last term in the total Lorentz number represents the ambipolar contribution to the thermal conductivity. The electronic contribution to the thermal conductivity is given by

$$K_e = \mathcal{L}\sigma T. \tag{20}$$

For the two scattering mechanisms considered here, the total relaxation time is given by

$$\tau^\pm = (\tau^{-1}_{l\pm} + \tau^{-1}_{i\pm})^{-1}, \tag{21}$$

with $\tau^{-1}_{l\pm}$ and $\tau^{-1}_{i\pm}$ representing the carrier scattering rates due to acoustic lattice vibrations and ionized impurities, respectively. The relaxation time of carriers due to acoustic lattice vibrations[33] can be written

$$\tau_{l\pm} = \frac{\pi\hbar^4 v^2 d}{\sqrt{2}E^2_\pm (m_\pm k_B T)^{3/2}} x^{-1/2}. \tag{22}$$

The relaxation time of carriers due to ionized impurities[32] can be written

$$\tau_{i\pm} = \frac{\sqrt{2m_\pm}\epsilon^2_\pm}{\pi e^4 N_d g_\pm}(k_B T)^{3/2} x^{3/2}, \tag{23}$$

with

$$g_{\pm} = \ln(1 + b_{\pm}) - \frac{b_{\pm}}{1 + b_{\pm}}, \tag{24}$$

$$b_{\pm} = \frac{\epsilon_{\pm} h}{e^2} \left(\frac{2k_B T}{m_{\pm}}\right)^{1/2} x/F_{-1/2}(\eta^*). \tag{25}$$

This completes the description of the model for the electrical properties.

IV. LATTICE THERMAL CONDUCTIVITY MODEL

Detailed models for the lattice thermal conductivity of doped silicon-germanium alloys have been presented previously.[3,30] The model due to Steigmeier and Abeles[30] is adopted here, with only minor modifications. In this model, the lattice contribution to the thermal conductivity is given by[34,35]

$$K_l = \frac{k_B}{2\pi^2 v} \left(\frac{k_B \theta}{\hbar}\right)^3 \left(I_1 + \frac{I_2^2}{I_3}\right), \tag{26}$$

where

$$I_1 = \int_0^{\theta/T} \tau_c \frac{x^4 \exp(x)}{[\exp(x) - 1]^2} dx, \tag{27}$$

$$I_2 = \beta \int_0^{\theta/T} \frac{\tau_c}{\tau_U} \frac{x^4 \exp(x)}{[\exp(x) - 1]^2} dx, \tag{28}$$

and

$$I_3 = \beta \int_0^{\theta/T} \frac{1}{\tau_U} \left(1 - \beta \frac{\tau_c}{\tau_U}\right) \frac{x^4 \exp(x)}{[\exp(x) - 1]^2} dx. \tag{29}$$

In these expressions, τ_c^{-1} is the total phonon-scattering rate, τ_u^{-1} is the phonon-scattering rate due to three-phonon umklapp processes, β is the ratio of the normal three-phonon-scattering rate to the umklapp three-phonon-scattering rate, and the integration variable is the reduced frequency, $x = \hbar\omega/k_B T$.

The umklapp three-phonon-scattering rate is given by[36]

$$\tau_u^{-1} = \frac{20\pi}{3} \hbar N_A \left(\frac{6\pi^2}{4}\right)^{1/3} \times \frac{1 + \frac{5}{9}\beta}{1 + \beta} \frac{\gamma^2}{Ma^2} \left(\frac{T}{\theta}\right)^3 x^2, \tag{30}$$

and the normal three-phonon-scattering rate is given by

$$\tau_N^{-1} = \beta \tau_u^{-1}. \tag{31}$$

Two additional scattering mechanisms are considered: scattering of phonons by point defects and scattering of phonons by charge carriers. The phonon-scattering rate due to point defects is given by[37]

$$\tau_{pd}^{-1} = y(1 - y) \left[\left(\frac{\Delta M}{M}\right)^2 + \epsilon_s \left(\frac{\Delta a}{a}\right)^2\right] \times \left(\frac{a}{v}\right)^3 \left(\frac{k_B T}{\hbar}\right)^4 x^4, \tag{32}$$

where ϵ_s is a strain parameter.

The phonon-scattering rate due to electron-phonon scattering is given by[38,39]

$$\tau_e^{-1} = \frac{E_{\pm}^2 m_{\pm}^3 v}{4\pi\hbar^4 d T_{\pm}^*} \times \ln\left(\frac{1 + \exp(-T_{s\pm}^* + \eta^* - x^2/16T_{s\pm}^* + x/2)}{1 + \exp(-T_{s\pm}^* + \eta^* - x^2/16T_{s\pm}^* - x/2)}\right), \tag{33}$$

where $T_{s\pm}^* = \frac{1}{2} m_{\pm} v^2/k_B T$ is the reduced carrier energy, at the speed of sound. The total phonon scattering rate is then given by

$$\tau_c^{-1} = (1 + \beta)\tau_u^{-1} + \tau_{pd}^{-1} + \tau_e^{-1}, \tag{34}$$

which completes the description of the lattice thermal conductivity model.

V. NUMERICAL DETAILS

The expressions described in Secs. II, III, and IV have been reduced to a computer code which allows calculation of the observable transport coefficients, given values for the independent parameters $\{y,T\}$ and the adjustable parameters $\{\beta,\gamma\epsilon_s,m_-,E_-,\epsilon_-,m_+,E_+,\epsilon_+,\eta^*\}$. The integrals are evaluated to a part in 10^{-6} using a published algorithm for Romberg's method.[40] The parameters β and γ describe the phonon scattering in undoped, unalloyed silicon and have been previously evaluated[30] as $\beta = 2.0$ and $\gamma = 0.91$. ϵ_s determines the contribution of strain disorder to point defect scattering of phonons and was previously estimated[30] as $\epsilon_s = 39$, and represents less than 9% of the $\Delta M/M$ term in any case.

This study has been restricted to SiGe alloys with carrier densities greater than 10^{18} cm^{-3}. The effect of minority carriers (holes) nevertheless becomes important at high temperatures in some cases, and the minority band must be modeled to even qualitatively reproduce the observed transport properties. Estimation of the valence-band parameters, $\{m_+,E_+,\epsilon_+\}$, however, will not be particularly reliable since by far most of the experimental results are dominated by the majority carriers (electrons). For simplicity, then, the electron and hole parameters have been taken as identical.

With these simplifications, the number of adjustable parameters is reduced to four: $\{m_{\pm},E_{\pm},\epsilon_{\pm},\eta^*\}$. Determination of the four observable transport coefficients $\{\sigma\mu_H,Q,K\}$ on a sample at a known composition and temperature $\{y,T\}$ is, therefore, sufficient to make an estimate of all four parameters, and all of the other transport properties can then be calculated.

An ideal experimental data point, then, would consist of the set $\{y_i,T_i;\sigma_i,\mu_{Hi},Q_i,K_i\}$, where i is an index to identify a data point. The three values $m_{\pm}$, $E_{\pm}$, and $\epsilon_{\pm}$ are taken to be independent of composition, temperature, and doping level. However, the chemical potential η_i^* will, in general, be different for each data point. Hence, there will be a total of $3 + N$ adjustable parameters, where N is the total number of data points used in the analysis.

The best-fit values for the adjustable parameter are determined by minimizing the function

$$\chi^2 = \sum_{i=1}^{N} W_i^{\sigma}\left(1 - \frac{\sigma_i}{\sigma_i^c}\right)^2 + \sum_{i=1}^{N} W_i^{\mu}\left(1 - \frac{\mu_i}{\mu_i^c}\right)^2 + \sum_{i=1}^{N} W_i^{Q}\left(1 - \frac{Q_i}{Q_i^c}\right)^2 + \sum_{i=1}^{N} W_i^{K}\left(1 - \frac{K_i}{K_i^c}\right)^2, \tag{35}$$

where the weighting factors $\{W^{\sigma},W^{\mu},W^{Q},W^{K}\}$ are either 1 or 0, depending on whether the corresponding experimental value is known or not, and the superscript c indicates the value of the transport coefficient calculated using $\{y_i,T_i;m_{\pm},E_{\pm},\epsilon_{\pm},\eta_i^*\}$. A generalization of Bevington's CURVEFIT routine was used for this purpose.[41]

The number of degrees of freedom, N_{DF}, indicates the extent to which a problem is overdetermined, and for this case is given by the number of independent pieces of experimental information plus 1, reduced by the number of adjustable parameters:

$$N_{\mathrm{DF}}=\sum_{i=1}^{N}W_i^{\sigma}+\sum_{i=1}^{N}W_i^{\mu}+\sum_{i=1}^{N}W_i^{Q}+\sum_{i=1}^{N}W_i^{K}+1-(3+N). \tag{36}$$

A consequence of the choice to optimize all η_i^* is that a data point consisting of only a single transport coefficient (say, σ_i alone, for example) will not contribute to the number of degrees of freedom or to the value of χ^2. This point will be further discussed in Sec. VII.

Experimental data were taken from several sources, which are summarized in Table II. The data cover a composition range from pure silicon to $Si_{0.63}Ge_{0.37}$, carrier densities from 10^{18} to 3×10^{20}, temperatures from 300 to 1300 K, and represents 151 independent measurements of transport coefficients with 90 degrees of freedom, for the determination of 61 adjustable parameters, 58 of which represent chemical potential values. In other words, the database represented in Table II contains 90 independent pieces of experimental information above and beyond the minimum number required to determine the 61 adjustable parameters. All of the data used in this study were determined on single-crystal or zone-leveled materials, with the exception of two hot-pressed SiGe/GaP samples which had large grains after extensive annealing at high temperatures.[14]

VI. RESULTS

A single least-squares fit simultaneously applied to all of the data described in Table II resulted in the values $m_{\pm}=1.40m_e$, $E_{\pm}=2.938$ eV, and $\epsilon_{\pm}=27.4$ with a root-mean-square deviation between the calculated and observed values of $\sqrt{\chi^2/N_{\mathrm{DF}}}=0.15$ or about 15%. Comparisons between the observed and calculated values for the electrical resistivity, Hall mobility, Seebeck coefficient, and thermal resistivity values are shown as functions of temperature in Figs. 1–3, respectively, for several representative samples of SiGe.

The model indicates that the drop in the electrical resistivity, Seebeck coefficient, and thermal resistivity at high temperatures for samples 68 and 41 is due to the intrinsic thermal excitation of holes. This is confirmed by the weak temperature dependence of the ionized donor density calculated for these samples, as shown in Fig. 4. At first sight, similar decreases in the electrical resistivity, Seebeck coefficient, and thermal resistivity for samples 162 and T373 might be attributed to intrinsic behavior also. But this model confirms that for these two very heavily doped samples, the ionized donor density is increased significantly at the highest temperatures, as was suggested previously[2] for sample 162.

Figure 5 shows a comparison between observed and calculated values for the Hall mobility as a function of ionized donor density. All of the qualitative trends exhibited by the experimental results are reproduced by the model, but the calculated Hall mobilities at the highest temperatures are as much as 37% higher than the observed values. The model also tends to overestimate the Seebeck coefficient values at low temperatures, by as much as 25% in the worst cases.

Figure 6 shows calculated values for the lattice thermal conductivity which decreases with increasing temperature and with increasing ionized donor density, as expected. Figure 7 shows the electronic thermal conductivity, the lattice thermal conductivity, and the total thermal conductivity as a function of doping level for n-type $Si_{0.80}Ge_{0.20}$ at 1300 K. The increase in K_e as the doping level decreases below 10^{20} cm^{-3} is due to the ambipolar contribution [third term in Eq. (19)].

Figure 8 shows calculated values for the thermoelectric fig-

TABLE II. Experimental data on SiGe alloys.

Number of samples	Composition range	Doping range (10^{19} cm^{-3})	Temperature range (K)	Data available
3[a]	0.0	1.2–10	300	σ,μ_H,Q[b]
1[c]	0.0	30	300	σ,μ_H,Q[b]
7[d,e]	0.15–0.37	2–15	300–1300	σ,Q,K
5[d]	0.2–0.3	8–22	300	σ,μ_H,Q,K
2[f]	0.2	20	300–1273	σ,Q
3[g]	0.0–0.2	15	300–1273	σ,μ_H,K

[a] Reference 42.
[b] Reference 32.
[c] Reference 43.
[d] Reference 2.
[e] Reference 44.
[f] Reference 14.
[g] This study.

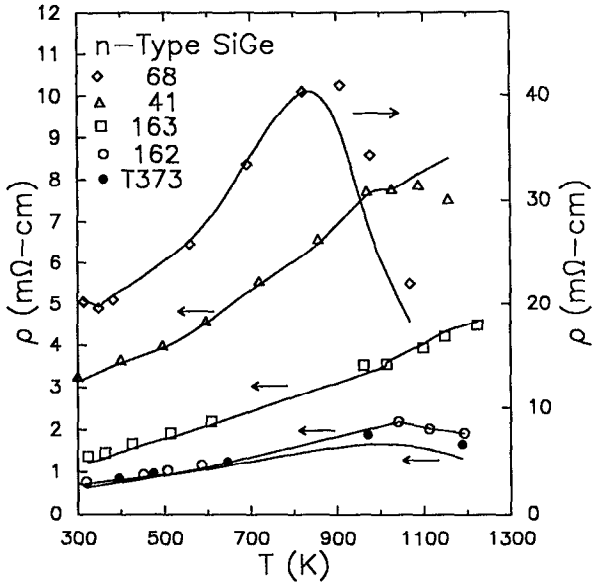

FIG. 1. The electrical resistivity as a function of temperature for five samples of n-type SiGe. The points represent experimental results, and the solid lines represent the model.

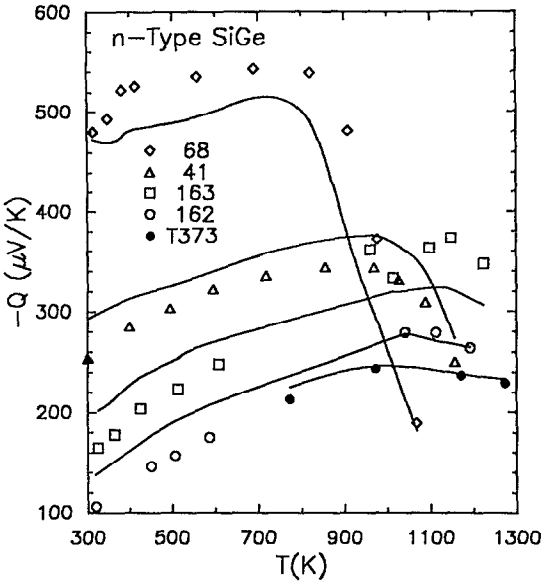

FIG. 2. The Seebeck coefficient as a function of temperature for five samples of *n*-type SiGe. The points represent experimental results, and the solid lines represent the model.

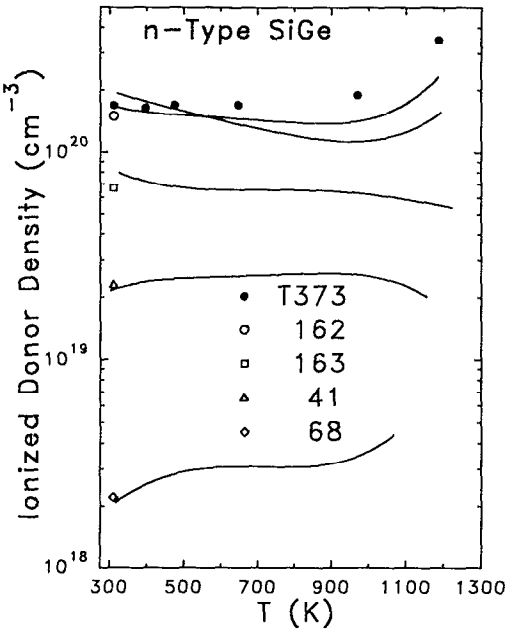

FIG. 4. The ionized donor density as a function of temperature for five samples of *n*-type SiGe. The points represent experimental results ($1/eR_H$), and the solid lines represent the model.

ure of merit, ZT, and the highest experimental values (sample T373) used in this study. Again, the model is in reasonable agreement with the experimental results and suggests that sample T373 has a figure of merit near the optimum value.

VII. DISCUSSION

The model presented provides a good description of the transport properties of heavily doped, *n*-type SiGe alloys. On average, the model can calculate any of the 151 independent, measured transport coefficients to within about $\pm$ 15%. Conversely, given a sample of known composition and doping level, the model can simultaneously and self-consistently predict all of the important transport coefficients with reasonable confidence. Variations of each of the transport properties with composition, doping level, and temperature are reproduced by the model with reasonable accuracy and a minimum of adjustable parameters. As an interpolation tool, as a starting point for understanding more complex situations, and as a framework for guiding future

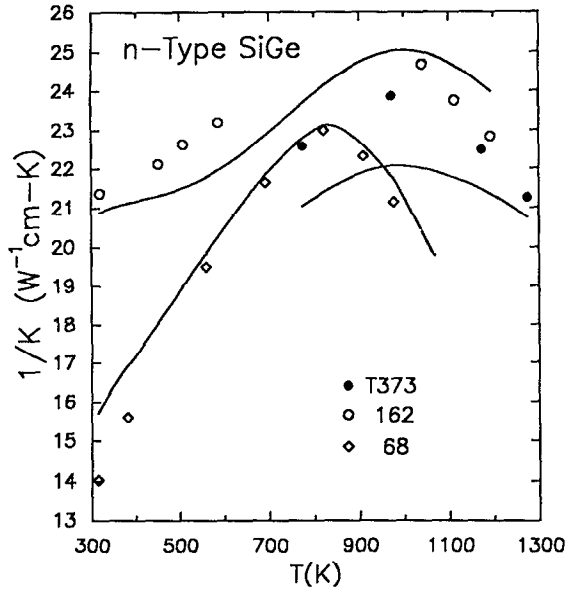

FIG. 3. The thermal resistivity as a function of temperature for three samples of *n*-type SiGe. The points represent experimental results, and the solid lines represent the model.

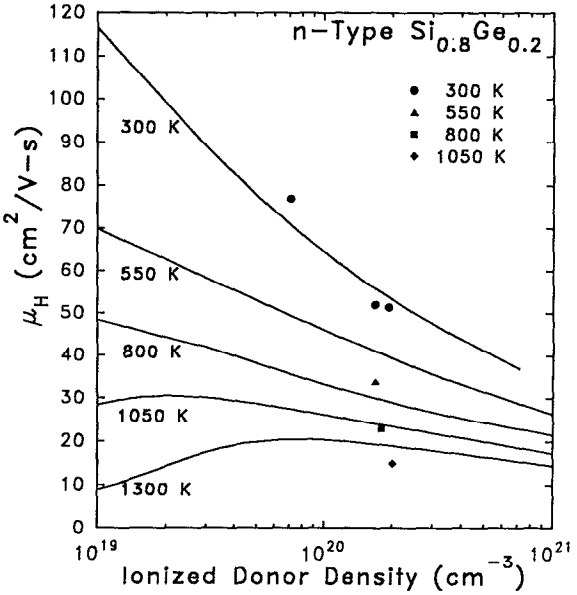

FIG. 5. The Hall mobility as a function of the ionized donor density for *n*-type SiGe. The points represent experimental results, and the solid lines represent the model.

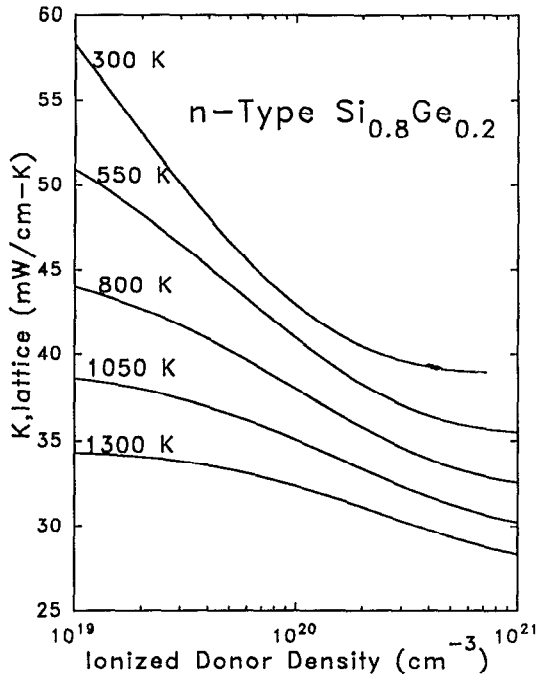

FIG. 6. The calculated lattice thermal conductivity as a function of ionized donor density and temperature for n-type $Si_{0.8}Ge_{0.2}$.

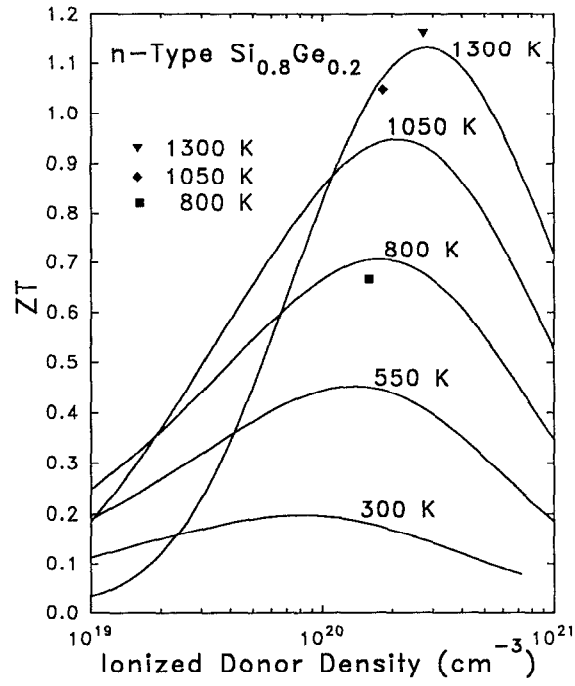

FIG. 8. The dimensionless thermoelectric figure of merit of n-type SiGe alloys as a function of ionized donor density. The three points represent experimental results on T373, a heavily annealed sample of SiGe/GaP.

experiments, the present model is expected to be quite useful. Nevertheless, the model is in many respects oversimplified, and extrapolation beyond the limits constrained by experimental data could be unreliable.

Before discussing the reliability of the results of this work, two related points will be discussed: the need to allow the chemical potential to be an adjustable parameter and effects neglected in this model.

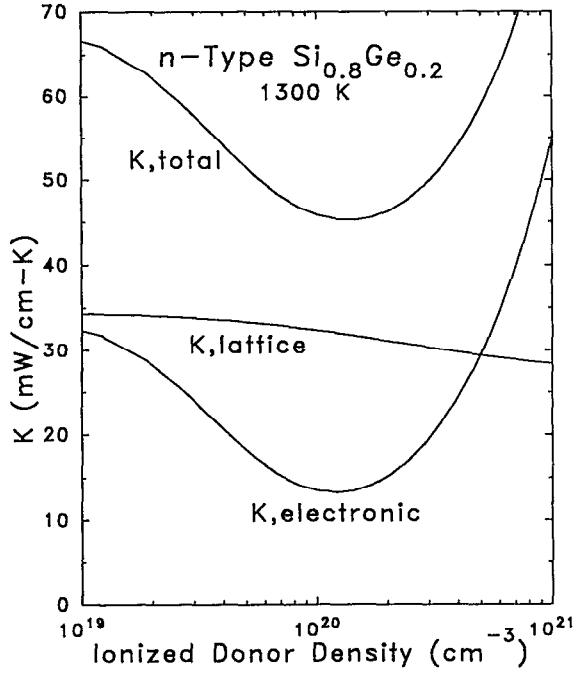

FIG. 7. The electronic (including ambipolar) thermal conductivity, lattice thermal conductivity, and total thermal conductivity as a function of ionized donor density for $Si_{0.8}Ge_{0.2}$ at 1300 K.

As noted above, a significant simplification of the model would result if all data points corresponding to a single sample were assumed to have a single, unique doping level. In this case, only a single piece of experimental information per sample (such as a single Hall-coefficient measurement) would be required to fix the chemical potential values for a given scattering mechanism by using the charge balance condition [Eq. (14)]. This assumption would reduce the number of chemical potential values which must be determined from the present case of one for each temperature at which a measurement has been performed to one for each sample which has been measured.

Unfortunately, the instability toward dopant precipitation of heavily doped, n-type SiGe alloys was noted even among the earliest investigations of these materials.[2,3] The precipitation of dopants from these supersaturated solutions has been well studied[23–25,45–47] and can occur at observable rates even during the normal course of characterization at high temperatures.[2] Ekstrom and Dismukes,[45] for example, reported an increase in the carrier concentration from about 7.5×10^{19} cm^{-3} to about 12.5×10^{19} cm^{-3} in about 12 min at 600 °C in an n-type SiGe sample. Shukla and Rowe[47] performed a more extensive study using high-temperature Hall-effect measurements which show that a 30% change in the carrier concentration in 60 min is not uncommon for these materials. That the number of dopants in solution depends not only on temperature, but also on the history of the sample, is an experimental fact which must be accounted for in any description of the high-temperature properties of these materials.

Thus, the precipitation and resolution of dopants *during* high-temperature transport measurements, which may take

many hours or even a few days to perform, preclude the assumption of constant doping level in heavily doped materials ($n > 10^{20}$ cm^{-3}). A quite distinct effect may be observed in less heavily doped materials, where a small (≈ 50 meV)[32] ionization energy means the dopants are not entirely ionized, as has been accounted for in models of the mobility in silicon.[29] It thus appears that there is at most only a very narrow range of doping levels for which the concentration of electrically active dopants, N_d, may be taken as constant.

Unfortunately, as noted in Sec. V, the need to estimate the chemical potential for each data point means that a measurement of a *single* transport coefficient is irrelevant, since even with all other parameters fixed, variation of the chemical potential alone will generally result in perfect agreement with the experimental values. This is to say that at least *two* transport coefficients must be known simultaneously, one of which will simply be "consumed" in the determination of the chemical potential.

One could, as is often done, simply use the measured Seebeck coefficient or Hall coefficient and simple expressions such as $S = -(k_B/e)(2 - \eta^*)$or $R_H = -1/eN_d$ to estimate the doping level or chemical potential. This would seem to substantially reduce the number of adjustable parameters and is operationally simple to perform. But these expressions are already approximations to Eqs. (5) and (6) which assume something about the scattering mechanisms and degree of degeneracy. Moreover, even this *is* a fitting procedure, although a trivial one.

The minimization procedure [Eq. (35)] used in this study is not really greatly different from the simpler approach, only more systematic. Seebeck-coefficient data and Hall-coefficient data still influence the estimate for the chemical potential far more strongly than either electrical conductivity or thermal conductivity data, just as in the simpler approach, but in this case all of the available experimental information are treated on an equal footing. In any case, the weak temperature dependence of the doping levels shown in Fig. 4 is typical of *n*-type SiGe alloys[45-47] and is reasonably consistent with the mechanisms described above, suggesting the fitting procedure used is not entirely unjustified.

While the major effects have been accounted for, as evidenced by the reasonable agreement with experiment, systematic errors in the Seebeck coefficient near room temperature and the mobility at high temperature certainly indicate that some significant effects have been neglected. Inclusion of *any* further effects would, due to the minimization procedure employed, produce better agreement with the data. For an indication of which effects should be incorporated into the model, some of the more important neglected effects will now be briefly discussed.

The energy and temperature dependence of several important electron-scattering mechanisms are summarized in Table III. Only the effects of intravalley scattering by acoustic phonons and scattering by ionized impurities have been included in this study. Calculations for the mobility of undoped silicon generally include optical-phonon scattering[48] in order to account for the faster than $T^{-3/2}$dependence of mobility in undoped silicon. To reproduce the composition dependence of the mobility of undoped $Si_{1-y}Ge_y$ alloys, alloy disorder scattering has been considered.[28] Alloy disorder scattering has the same energy dependence as intravalley acoustic-phonon scattering, but yields a mobility proportional to $T^{-1/2}$. Neutral impurity scattering

TABLE III. Approximate ϵ and T dependencies for electron-scattering mechanisms.

Scattering mechanism	Energy dependence of $\tau\tau$	Temperature dependence of $\mu^{nondegen}\mu^{degen}$	
Intravalley acoustic phonons	$\epsilon^{-1/2}$	T^{-1}	$T^{-3/2}$ T^{-1}
Intervalley optical phonons	$\epsilon^{-1/2}$	T^{-1}	$T^{-3/2}$ T^{-1}
Ionized impurities	$\epsilon^{3/2}$	T^{0}	$T^{3/2}$ T^{0}
Alloy disorder	$\epsilon^{-1/2}$	T^{0}	$T^{-1/2}$ T^{0}
Neutral impurities	ϵ^{0}	T^{0}	T^{0} T^{0}

(due to incompletely ionized dopants) has also been considered,[29] and recent calculations indicate intervalley acoustic-phonon scattering may be more important than intravalley scattering.[49]

Slack[50] has recently pointed out that even in silicon-rich alloys at sufficiently high doping levels, the four equivalent *L*-point conduction-band valleys will begin to be occupied. To account for this effect, additional band-structure parameters (masses and energies) as well as scattering-rate parameters for the *L*-point valleys would be required. Other effects such as the possible variation of the band gap with doping level[29] and the inequivalence of the electron and hole parameters have also been neglected here.

Phonon-drag effects, often large at low temperatures in silicon,[51] are generally reduced by alloying and increasing temperature.[52] Erofeev, Iordanishvili, and Petrov[3] argue that phonon-drag effects in the thermopower are not observed in silicon-germanium and concluded from this that electron-phonon scattering is not a major contributor to the phonon-scattering rate. The phonon-scattering model used here, essentially due to Steigmeier and Abeles, includes a significant electron-phonon contribution to phonon scattering, but neglects phonon-drag effects entirely.

The distinct various contributions of transverse acoustic, longitudinal,[53] and optical phonons[54] to the lattice thermal conductivity have been discussed and can be significantly different from the present model. More accurate expressions for the electron-phonon-scattering rate are available which account for many-valley band structures[55] and effective-mass anisotropy.[56] Also, departure of the high-temperature heat capacity of silicon and silicon-germanium from the simple Dulong–Petit value due to anharmonicity has not been reflected in the thermal conductivity calculations in any way.

Finally, we should point out the possibility that solutions to Boltzmann's equation assumed in the derivations of the transport coefficients used here, and even the very applicability of Boltzmann's equation itself, are in some question for both the electrons and phonons. Figure 9, for example, indicates that the electron mean free path at 1300 K is quite short, even less than the atomic size for a significant number of low-energy electrons. It should be recalled here that the model somewhat *overestimates* the mobility at high temperatures, and so the actual electron mean free path is shorter still.

The weighted-phonon mean free path is also only a few atomic diameters long, as shown in Fig. 10. Such small mean-

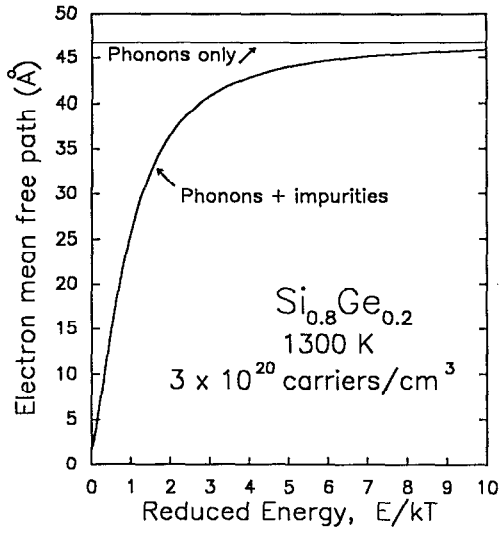

FIG. 9. Energy-dependent mean free path for electrons in n-type $Si_{0.8}Ge_{0.2}$ at 1300 K.

free-path values may be taken as a sign that perturbation theory expressions for the scattering rates should, at the least, be somewhat suspect. Cutoff procedures to prevent phonon mean-free-path values from getting too short have been suggested[54,57] mostly retain the simplicity of the present lattice thermal conductivity calculations, yield good agreement with experiment[58] and are physically reasonable, but do not directly address the breakdown of perturbation theory for very high scattering rates.

The exceedingly small mean-free-path values that come from this analysis is a warning sign that the Boltzmann equation approach may not be reliable and some other, more powerful formalism altogether might be considered for analyzing these heavily doped semiconductor alloys. A self-consistent, first-principles calculation using a formally more correct transport property calculation scheme (such as the Kubo formalism) for the coupled electron-phonon system appropriate to heavily doped semiconductor alloys would be a welcome contribution, but has not yet been performed. The qualitative variation of the transport properties with temperature, doping level, and/or composition, however, is not expected to be qualitatively different from the present model.

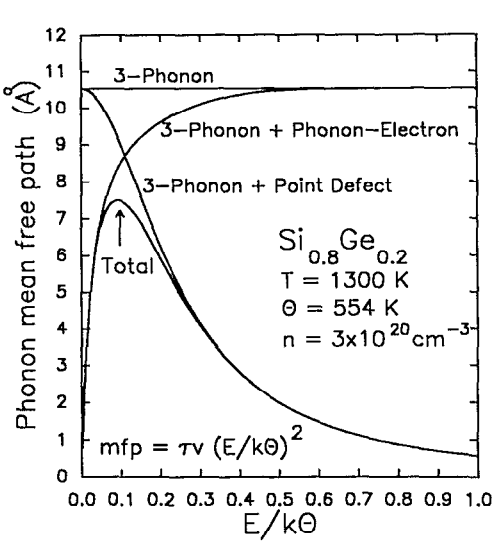

FIG. 10. Energy-dependent mean free path for phonons in n-type $Si_{0.8}Ge_{0.2}$ at 1300 K, weighted as for thermal conductivity calculations.

That the simplistic model adopted here fails in some ways is, therefore, not remarkable. Indeed, considering the neglected effects, the agreement with experiment is somewhat remarkable. Moreover, the values of the adjustable parameters determined in this study, $\{m_{\pm}, E_{\pm}, \epsilon_{\pm}\}$, should be regarded as "effective values," since these parameters have been required to "absorb" so many effects not explicitly modeled.

Comparison to literature values for the adjustable parameters is of some interest, but complicated by use of different forms for relaxation times and different values for dependent parameters. The effective mass and deformation values determined here are physically reasonable, but differ significantly from the values of Li and Thurber (who also used a different value for the speed of sound). This difference is highlighted by calculating the acoustic-phonon contribution to the conductivity mobility μ_a, which in the nondegenerate limit is given by

$$\mu_a = \frac{2(2\pi)^{1/2} e\hbar^4 d v^2}{3m_-^{5/2}(k_B T)^{3/2} E_-^2}. \tag{37}$$

Table IV compares the parameters used and calculated values for μ_a at 300 K in silicon. The much lower value for μ_a found in this study indicates that the model described here seriously underestimates the mobility of intrinsic materials, a natural result of the database which included only heavily doped materials (see Table II).

A difficulty associated with the Brooks–Herring scattering rate for impurity scattering [Eqs. (23)–(25)] is the uncertainty over the choice of the appropriate effective mass[29] for nonspherical electron energy surfaces. Long[59] concluded that the Brooks–Herring ionized-impurity scattering rate was reliable only if the effective mass was taken as an adjustable parameter. The large value for the dielectric constant deduced here, $\epsilon_{\pm} = 27.4$ compared to 11.7 used by Li and Thurber, similarly reflects the uncertainty in assigning values to the important parameters of the model.

The generally close agreement between experiment and the model suggests that the major energy and temperature dependencies of the scattering rates are modeled reasonably well. The electrical mobility, however, is underestimated for low doping levels (less than 10^{18}) and overestimated at high temperatures ($T > 1000$ K). Also, the Seebeck coefficient is generally overestimated at low temperatures (300 K). These discrepancies indicate that the model is too simple in important respects.

TABLE IV. Acoustic-phonon contribution to the conductivity mobility.

	m/m_e	$E_{\pm}$ (eV)	v (cm/s)	μ_a (300 K) (cm^2/V s)
This study	1.40	2.938	5.88×10^5	243
Li and Thurber	0.30	12.8	9.2×10^5	1503

That the calculated mobility at high doping levels decreases at high temperature too slowly cannot be remedied by including any of the scattering rates discussed, since the acoustic-phonon mobility decreases with temperature as fast or faster than any of the other mechanisms (see Table III). The calculated temperature dependence could be increased by increasing the contribution of acoustic scattering rate relative to the ionized-impurity scattering rate, but this would *decrease* the calculated mobility at low carrier density, exacerbating an already poor agreement with experiment.

It seems unlikely, then, that including more scattering mechanisms will remove the major discrepancies between the model and experiment. Better agreement with experiment could, of course, be achieved if the parameters are allowed to vary with temperature and/or doping level. An alternative approach is to assume that the carriers can be divided into two types: (1) electrons in the conduction band and (2) electrons in the impurity band. Each type of carrier would then have its own effective mass, deformation potential, and dielectric constant, and the additional flexibility can reproduce a much wider range of behavior.

Support for this idea comes from consideration of the density of impurity atoms. On the assumption that the carrier concentrations calculated with Eqs. (1), (9), and (14) are all in the conduction band, then N_d represents the number of *ionized* impurities. The total density of impurity atoms, N_{total}, is given by

$$N_d = \frac{N_{\text{total}}}{2e^{\eta^*} + 1}, \tag{38}$$

in this case and is shown in Fig. 11, calculated using $m_{\pm} = 1.4 m_e$. The total donor density needed to achieve $N_d = 2\times10^{20}\ \text{cm}^{-3}$ is about $N_{\text{total}} = 2\times10^{22}\ \text{cm}^{-3}$, which is clearly an unphysical result. And a smaller effective-mass value only makes the total number of impurities needed to achieve a particular density of carriers in the conduction band even larger.

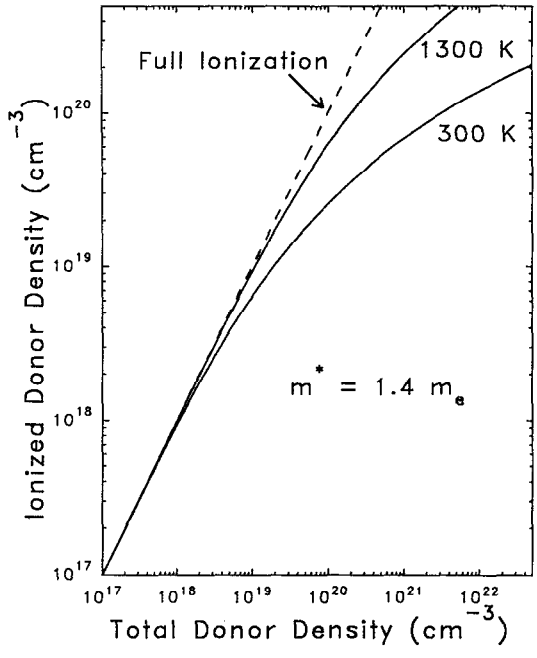

FIG. 11. Ionized donor density as a function of total donor density, assuming that the impurity states are localized.

The reason for this is that the impurity states are not localized, but have formed an itinerant impurity band[60] (and/or merged with the conduction band), and at very high doping levels most of the carriers actually occupy states derived from the impurity bands. In this case, there is no reason why the parameters describing transport in the impurity band should be the same as the parameters describing the conduction band. It may be possible, then, to extend the present model to low carrier concentrations ($n \ll 10^{18}\ \text{cm}^{-3}$) by incorporating an additional band with scattering parameters typical of the conduction band of lightly doped silicon, with the division of carrier densities between the two bands determined by Eq. (38).

VIII. CONCLUSIONS

The high-temperature transport properties of heavily doped, *n*-type silicon-germanium alloys are reasonably well described using conventional Boltzmann expressions for the transport coefficients. The principal value of the model is not in its rigor (which is imperfect) or in its accuracy (which is good, but not astounding). The principal value of this model is that it provides a tool which reliably predicts all of the qualitative trends as functions of composition, doping level, and temperature in a reasonably accurate and internally consistent manner. Only two scattering mechanisms (acoustic phonon and ionized acoustic scattering) are needed to describe the electrical transport, and only three scattering mechanisms (phonon-phonon, point defect, and electron-phonon scattering) are required to describe the phonon transport. The parameters describing the electrical transport, however, are significantly different from parameters typical of lightly doped silicon and imply that the impurity states are not localized, but form extended, nearly free electron states. It is suggested that this model, valid for high doping levels, can be reconciled with the observed properties at low doping densities by partitioning the carriers into lighter, conduction-band carriers and heavier, impurity-band carriers, with different parameters describing each band.

ACKNOWLEDGMENTS

The author would like to thank Dr. G. Slack, Dr. P. Klemens, and Dr. C. Wood for many helpful discussions related to this work. The work described in this paper was carried out at the Jet Propulsion Laboratory, California Institute of Technology, under contract with the National Aeronautics and Space Administration.

[1] B. Abeles, D. S. Beers, G. D. Cody, and J. P. Dismukes, Phys. Rev. **125**, 44 (1962).
[2] J. P. Dismukes, L. Ekstrom, E. F. Steigmeier, I. Kudman, and D. S. Beers, J. Appl. Phys. **35**, 2899 (1964).
[3] R. S. Erofeev, E. K. Iordanishvili, and A. V. Petrov, Sov. Phys. Solid State **7**, 2470 (1966)
[4] P. R. Sham and L. H. Gnau, Z. Metalkd. **59**, 137 (1968).
[5] C. B. Vining, W. Laskow, J. O. Hanson, R. R. Van der Beck, and P. D. Gorsuch to be published in J. Appl. Phys.
[6] G. L. Bennett, J. J. Lombardo, and B. J. Rock, in Proceedings of the 18th International Energy Conversion Engineering Conference, Orlando, FL, 1983.
[7] D. M. Rowe, J. Power Sources **19**, 247 (1987).
[8] M. I. Alonso and E. Bauser, J. Appl. Phys. **62**, 4445 (1987).

[9] V. F. Kukoz, V. N. Lozovskii, and V. P. Popov, Inorg. Mater. **24**, 1178 (1988).
[10] Q. Z. Hong, J. G. Zhu, and J. W. Mayer, J. Appl. Phys. **55**, 747 (1989)
[11] K. Murase, A. Takeda, and Y. Mizushima, Jpn. J. Appl. Phys. **21**, 561 (1982).
[12] S. Kodato, J. Non-Cryst. Solids **77&78**, 893 (1985).
[13] C. M. Bhandari and D. M. Rowe, Contemp. Phys. **21**, 219 (1980).
[14] J. W. Vandersande, C. Wood, and S. Draper, Mater. Res. Soc. Symp. Proc. **97**, 347 (1987).
[15] J. W. Vandersande, A. Borshchevsky, J. Parker, and C. Wood, in *Proceedings of the 7th International Conference on Thermoelectric Energy Conversion*, edited by K. R. Rao (University of Texas, Arlington, TX, 1988), p. 76.
[16] M. A. A. Issa, F. A. A. Amin, A. M. Hassib, and Z. H. Dughaish, J. Mater. Sci. **24**, 2300 (1989).
[17] P. K. Pisharody and L. P. Garvey, in *Proceedings of the 7th Intersociety Energy Conversion Engineering Conference* (IEEE, New York, 1978), p. 1963.
[18] H. J. Goldsmid and A. W. Penn, Phys. Lett. **27A**, 523 (1968).
[19] D. M. Rowe, J. Phys. D **7**, 1843 (1974).
[20] D. M. Rowe, and V. S. Shukla, J. Appl. Phys. **52**, 7421 (1981).
[21] D. M. Rowe, V. S. Shukla, and N. Savvides, Nature **290**, 765 (1981).
[22] H. R. Meddins and J. E. Parrott, J. Phys. C **9**, 1263 (1976).
[23] V. Raag, in *Proceedings of the 10th Intersociety Energy Conversion Engineering Conference* (IEEE, New York, 1975), p. 156.
[24] V. Raag, in *Proceedings of the 11th Intersociety Energy Conversion Engineering Conference* (IEEE, New York, 1976), p. 1527.
[25] V. Raag, in *Proceedings of the 2nd International Conference on Thermoelectric Energy Conversion*, edited by R. K. Rao (University of Texas, Arlington, TX, 1983), p. 5.
[26] G. Stapfer and V. Truscello, in *Proceedings of the 11th Intersociety Energy Conversion Engineering Conference* (IEEE, New York, 1976), p. 1533.
[27] A. Amith, in *Proceedings of the 7th International Conference on the Physics of Semiconductors*, edited by M. Hulin (Academic, New York, 1964), p. 393.
[28] S. Krishnamurthy, A. Sher, and A. Chen, Appl. Phys. Lett. **47**, 160 (1985).
[29] S. S. Li and W. R. Thurber, Solid-State Electron. **20**, 609 (1977).
[30] E. F. Steigmeier and B. Abeles, Phys. Rev. **136**, A1149 (1964).
[31] S. Krishnamurthy, A. Sher, and A. Chen, Phys. Rev. B **33**, 1026 (1986).
[32] V. I. Fistul, *Heavily Doped Semiconductors* (Plenum, New York, 1969).
[33] W. Shockley and J. Bardeen, Phys. Rev. **77**, 388 (1950).
[34] J. Callaway, Phys. Rev. **113**, 1046 (1959).
[35] J. Callaway and H. C. von Bayer, Phys. Rev. **120**, 1149 (1960).
[36] P. G. Klemens, in *Solid State Physics*, edited by F. Seitz and D. Turnbull (Academic, New York, 1958), Vol. 7, p. 1.
[37] P. G. Klemens, Phys. Rev. **119**, 507 (1960).
[38] J. M. Ziman, Philos. Mag. **1**, 191 (1956).
[39] J. M. Ziman, Philos. Mag. **2**, 292 (1957).
[40] *Numerical recipes in C* W. H. Press, B. P. Flannery, S. A. Teukolsky, and W. T. Vetterling (Cambridge University, Cambridge, England, 1988).
[41] P. R. Bevington, *Data Reduction and Error Analysis for the Physical Sciences* (McGraw-Hill, New York, 1969).
[42] W. R. Thurber, R. L. Mattis, Y. M. Lin, and J. J. Filliben, J. Electrochem. Soc. **127**, 1807 (1980).
[43] S. Solmi, M. Severi, R. Angelucci, L. Baldi, and R. Bilenchi, J. Electrochem. Soc. **129**, 1811 (1982).
[44] "Silicon Germanium Thermoelectric Materials and Module Development Program," topical report prepared under U.S. Atomic Energy Commission Contract No. AT(29-2)-2510, 1969.
[45] L. Ekstrom and J. P. Dismukes, J. Phys. Chem. Solids **27**, 857 (1966).
[46] E. L. Burgess and R. D. Nasby, J. Appl. Phys. **45**, 2375 (1974).
[47] V. S. Shukla and D. M. Rowe, Appl. Energy **9**, 131 (1981).
[48] D. Long, Phys. Rev. **120**, 2024 (1960).
[49] G. K. Schenter and R. L. Liboff, Phys. Rev. B **40**, 5624 (1989).
[50] G. Slack (private communication).
[51] T. H. Geballe and G. W. Hull, Phys. Rev. **98**, 940 (1955).
[52] D. K. C. MacDonald, *Thermoelectricity* (Wiley, New York, 1962).
[53] N. Savvides and H. J. Goldsmid, J. Phys. C **13**, 4671 (1980).
[54] G. Slack, Solid State Phys. **34**, 1 (1979).
[55] T. Sota and K. Suzuki, J. Phys. C **15**, 6991 (1982).
[56] T. Sota and K. Suzuki, J. Phys. C **16**, 4347 (1983).
[57] M. C. Roufosse and P. G. Klemens, J. Geophys. Res. **79**, 703 (1974).
[58] D. C. Cahill and R. O. Pohl, Solid State Commun. **70**, 927 (1989).
[59] D. Long, Phys. Rev. **129**, 2464 (1963).
[60] N. F. Mott, Philos. Mag. B **58**, 369 (1988).